



This is the accepted manuscript made available via CHORUS. The article has been published as:

Spectral phase singularity and topological behavior in perfect absorption

Mengqi Liu, Weijin Chen, Guangwei Hu, Shanhui Fan, Demetrios N. Christodoulides, Changying Zhao, and Cheng-Wei Qiu

Phys. Rev. B **107**, L241403 — Published 8 June 2023

DOI: [10.1103/PhysRevB.107.L241403](https://doi.org/10.1103/PhysRevB.107.L241403)

Spectral phase singularity and topological behaviors in perfect absorption

Mengqi Liu^{1,2}, Weijin Chen², Guangwei Hu³, Shanhui Fan³, Demetrios N. Christodoulides⁴,
Changying Zhao^{1*}, Cheng-Wei Qiu^{2*}

¹*Institute of Engineering Thermophysics, MOE Key Laboratory for Power Machinery and Engineering,
School of Mechanical Engineering, Shanghai Jiao Tong University, Shanghai 200240, China*

²*Department of Electrical and Computer Engineering, National University of Singapore, Singapore
117583, Singapore*

³*Department of Electrical Engineering, Ginzton Laboratory, Stanford University, Stanford, California
94305, USA*

⁴*Center for Research and Education in Optics and Lasers (CREOL), The College of Optics and
Photonics, University of Central Florida, Orlando, Florida 32816, USA*

* Email: changying.zhao@sjtu.edu.cn; chengwei.qiu@nus.edu.sg

Abstract

Perfect absorbers, which can achieve total absorption of all incoming energy, have been extensively studied in the last decades for various important technologies in general wave systems. Here we show that perfect absorption is generically associated with topological spectral phase singularity (SPS), carrying conserved and tunable quantized topological invariants in spectral space. The order of topological invariant $\tilde{\nu}$ depends on the number of degenerate outgoing channels. Two commonly-studied absorbers, mirror-backed and all-dielectric structures, are re-examined from a topological perspective, to reveal the generation, evolution, and annihilation of SPSs with $\tilde{\nu} = \pm 1$ or even high orders (i.e, $\tilde{\nu} = \pm 2, \pm 4$). A novel strategy based on charge conservation of SPSs to design dual-band perfect absorbers has been established. Our findings establish the topological origin of the robust existence of perfect absorption. More broadly, our work highlights topology as the fundamental property of conventional scattering behaviors. This insight could lead to new opportunities in applications such as biosensing, topological metasurfaces, micro/nano thermal radiation, etc.

Main text:

Absorption of light represents one of the most fundamental aspects of light-matter interactions. Over the last decades, many efforts have been dedicated to designing perfect absorbers [1] in nearly every part of the whole electromagnetic spectrum [2–6], motivated by applications in high-precisely sensing [7], photovoltaic/photothermic devices [8–10], super-resolution imaging [11,12], cloaking [13] and so on. Recently, benefiting from the great development of advanced nanofabrication technologies and in-depth research of photonic theories, various kinds of configurations have been proposed, including Dallenbach and Sailsbury absorbers [14], photonic crystals [15], multilayers [16], metal-insulator-metal (MIM) or hyperbolic metamaterials [17,18], all-dielectric metasurfaces [19], or even coherent perfect absorbers [20,21]. However, despite extensive studies in theories, structure design, multifunctional properties, or even active devices, the underlying topological behavior of perfect absorption has seldom been discussed.

Theoretically, perfect absorption (PA) ensures that all the incoming energy can be thoroughly absorbed without any scattering event. For extensively-studied mirror-backed perfect absorbers, for example, the PA can be generally achieved when the only reflection channel is completely suppressed. Before, such zero-reflection points were reported associated with a phase jump in the 1D reflection phase graph [22–25], but locking up exciting topological phenomena. More recently, by extending the view of reflection phase spectra into 2D spectral-parameter spaces, phase vortex described by non-zero topological charges, namely spectral phase singularities (SPSs) here, could be observed [14,26–30], which then been verified in different systems composed of metal arrays [14], atomically thin 2D materials [28], or epsilon-near-zero materials [31]. Our previous work focused on the evolution of reflection phase singularity pairs (zero reflection) in one-port systems [31], where PA could always be observed at this singular phase. However, it should note that all the above findings, including PA points and SPSs, are occasionally found by random parameter sweep for some specific configurations. Then, one open question may arise: *Can all perfect absorption in general be topological?* It, thereby, inspires us to re-think the underlying physics between PA and topology in a

more general view, to provide a universal design principle for PA via involving SPSs. An intuitive understanding of why such SPSs exist and are robust was previously lacking, and there is no general physical description of such PA-related SPSs. Besides, although a +2 SPS has been reported in the synthetic phase [28], i.e., $\arg(r_p / r_s)$ (r_p, r_s being reflection coefficients under p or s polarization), the explicit generation rule of higher-order SPSs and their connections between perfect absorbers have never been revealed yet.

In this work, we first re-interpret PA from a topological perspective based on temporal coupled-mode theory (TCMT) [32,33]. The generic principles to identify the order of SPSs at PA points are explicitly established, providing a universal guideline of designing perfect absorbers in different systems. The generation, evolution, and annihilation of SPSs with different orders have been analyzed in widely-studied absorbers. Further, the revealed topological behaviors of PA-associated SPSs also stimulate us to establish a new method to design dual-band perfect absorbers. The topological robustness of PA in other parameter spaces and the possibility of achieving other orders of SPSs are also discussed.

To build a general view, we begin with a multi-port system ($N=2n$ channels) in Fig. 1(a), which has a mirror symmetry and supports m resonant modes. Based on TCMT, one can obtain the scattering matrix [34]

$$\mathbf{S}=\mathbf{C}\left[\mathbf{I}-\frac{\mathbf{D}^*\mathbf{D}^T}{i(\omega-\boldsymbol{\Omega})+\boldsymbol{\Gamma}_e+\boldsymbol{\Gamma}_a}\right]=\begin{bmatrix} \mathbf{S}_{(U,U)} & \mathbf{S}_{(U,D)} \\ \mathbf{S}_{(D,U)} & \mathbf{S}_{(D,D)} \end{bmatrix} \quad (1)$$

where \mathbf{C} is a $N\times N$ matrix describing the scattering process without resonances, \mathbf{D} denotes the coupling matrix between resonances (frequency $\boldsymbol{\Omega}=[\omega_1, \omega_2, \dots, \omega_l, \dots, \omega_m]^T$) and outgoing channels. The $\boldsymbol{\Gamma}_e=[\Gamma_e^1, \Gamma_e^2, \dots, \Gamma_e^l, \dots, \Gamma_e^m]^T$ and $\boldsymbol{\Gamma}_a=[\Gamma_a^1, \Gamma_a^2, \dots, \Gamma_a^l, \dots, \Gamma_a^m]^T$ present the radiative loss and non-radiative (material) loss of the systems, respectively. The U_X, D_Y mark the X -th upper and Y -th down channels. Being constrained by reciprocity, there are $S_{(U_X, D_Y)}=S_{(D_Y, U_X)}$ and $S_{(U_X, U_Y)}=S_{(D_X, D_Y)}$ ($X, Y \in [1, n]$). Here we

merely consider incident light from the upper plane, then the scattering matrix reduces to $\mathbf{S} = [\mathbf{S}_{(U,U)}, \mathbf{S}_{(U,D)}]$, where the element $S_{(U_x, U_y)}$ [$S_{(U_x, D_y)}$] reads reflection (transmission) coefficients account for light transporting from U_x to U_y (D_y). Then, absorption can be calculated by energy conservation: $A = 1 - \sum_{X=1}^n \sum_{Y=1}^n [|S_{(U_x, U_y)}|^2 + |S_{(U_x, D_y)}|^2]$, so that every matrix element of \mathbf{S} being zero is both necessary and sufficient to create PA ($A = 1$). The degenerate zeros are associated with ill-defined points in the transmission phase $\varphi_{t_{x,y}} = \arg[S_{(U_x, D_y)}]$ and reflection phase $\varphi_{r_{x,y}} = \arg[S_{(U_x, U_y)}]$. PA thus in general corresponds to a set of degenerate SPSs.

We suppose that resonant modes are orthogonal unless otherwise stated, then one can obtain elements in Eq. (1) expressed by

$$S_{(U_x, D_y)} = \delta_{x,y} \tilde{t}_x - \sum_{l=1}^m \frac{\beta_l \cdot \tilde{r}_x \gamma_e^l + \tilde{t}_x \gamma_e^l}{i(\omega - \omega_l) + \Gamma_e^l + \Gamma_\alpha^l} \quad (2-1)$$

$$S_{(U_x, U_y)} = \delta_{x,y} \tilde{r}_x - \sum_{l=1}^m \frac{\tilde{r}_x \gamma_e^l + \beta_l \cdot \tilde{t}_x \gamma_e^l}{i(\omega - \omega_l) + \Gamma_e^l + \Gamma_\alpha^l} \quad (2-2)$$

where \tilde{r}_x and \tilde{t}_x are the direct reflection and transmission coefficients in \mathbf{C} . We assume that the coupling efficiency between l -th mode and different channels are the same, hence $\gamma_e^l = 2\Gamma_e^l / N$. The mode parity is encoded in $\beta_l = \pm 1$ (+1 for symmetric modes, -1 for asymmetric modes). $\delta_{x,y}$ is the Dirac function. The details of derivation can be found in Supplemental Materials [34]. In the following, two basic perfect absorbers with different ports are considered to reveal the underlying topological behaviors.

One of the most commonly-studied perfect absorbers is mirror-backed structures with no diffraction in Fig. 1(b). The upper structure could be shaped using metamaterials or metasurfaces [3,42,43]. In this system ($N=1$), PA could be achieved if and only if there is only one resonant mode ($m=1, \omega_0$) [44]. Then, Eq. (2) is simplified

to $r_0 = S_{(u_1, v_1)} = \frac{-i(\omega - \omega_0) + \Gamma_e - \Gamma_\alpha}{i(\omega - \omega_0) + \Gamma_e + \Gamma_\alpha}$, $t_0 \equiv 0$. The reflection phase in $\omega - \Gamma_e / \Gamma_\alpha$ space

is given in Fig. 1(c). There is a phase vortex located exactly at $\omega = \omega_0, \Gamma_e = \Gamma_\alpha$ known as critical coupling condition [45] predicting the presence of PA. *Although this condition has been proposed for many years, the phase evolution and topological properties around this critical point in spectral space have seldom been discussed.* By tracing an anticlockwise closed loop around the singularity, a total accumulated phase of $+2\pi$ can be obtained, implying an integer winding number $\nu = +1$ calculated by

$$\nu = \frac{1}{2\pi} \oint d\varphi, \nu \in Z \quad (3)$$

with φ being the reflection phase $\varphi_0 = \arg(r_0)$ in this case. Similar definitions of topological invariants can also be found in describing bound states in the continuum (BICs) in momentum space [46–48], topological defects of 2D spins [49], spatial vortex beams [50,51], etc. Such findings reveal that topological nature is also inherently prevalent for PA at critical coupling since the annihilation of PA-related SPSs is only possible when topological charges of an opposite sign are present. Some works have already studied ± 1 phase singularities for specific cases [14,52], where the topological charges are created in, i.e., frequency-period or frequency-incident spaces, but the intrinsic connection between SPSs and design parameters is not well known yet. Here, we reveal that underlying the detailed tuning of the geometric parameters of structures, the key factor in generating SPS is the competitive balance of radiative loss (Γ_e) and non-radiative loss (Γ_α) of the system. In Figs. 1(d)-(g), we give several pictures with different shapes of $\Gamma_e(sp)$ and $\Gamma_\alpha(sp)$ at $\omega = \omega_0$, where “*sp*” represents a system parameter like thickness, period, or incident angle that influence the competitive values of $\Gamma_{e,\alpha}$. Fig. 1(d) shows a similar situation in Fig. 1(c), where a +1 SPS arises when the system changes from *overdamped* ($\Gamma_\alpha > \Gamma_e$) to *underdamped* ($\Gamma_\alpha < \Gamma_e$). As the

profile of Γ_e becomes parabolic in Fig. 1(e), there is another -1 SPS (*underdamped* \rightarrow *overdamped*). By moving the Γ_α down, two opposite SPSs will move synchronously and merge at the critical position in Fig. 1(f). In analogy with merging BICs [53], the magnitude of absorptivity still tends to $A \rightarrow 1$ as long as $\Gamma_\alpha \neq 0$. Particularly, the case of $\Gamma_\alpha = 0$ corresponds to the appearance of BIC in photonic systems. Afterward, the annihilation of two SPSs happens with no PA when the Γ_α further moves down [Fig. 1(g)].

When more channels are involved in the scattering process, the condition of PA corresponds to a set of degenerate SPSs, and the associated topological invariant \tilde{v} shows as

$$\tilde{v} = \sum_{X,Y=1}^n [p_{X,Y} \cdot v_{(U_X,U_Y)} + q_{X,Y} \cdot v_{(U_X,D_Y)}] = N \cdot v_{(U_1,U_1)} \quad (4)$$

where $p_{X,Y} = v_{(U_1,U_1)} / v_{(U_X,U_Y)}$ and $q_{X,Y} = v_{(U_1,U_1)} / v_{(U_X,D_Y)}$ are the signs of SPSs obtained for different channels in the same spectral space. The high-order SPS with \tilde{v} can be

observed by checking the phase of $\varphi = \arg \left[\prod_{X,Y=1}^n \left(S_{(U_X,U_Y)} \right)^{p_{X,Y}} \left(S_{(U_X,D_Y)} \right)^{q_{X,Y}} \right]$ with

$p_{X,Y}, q_{X,Y} = \pm 1$. For example, as for a two-port absorber ($N=2$) in Fig. 2(a), there are two resonant modes: asymmetric (label “a”) and symmetric (label “s”) modes. Thus,

Eq. (2) reduces to $t = S_{(U_1,D_1)} = 1 - \frac{\Gamma_e^a}{i(\omega - \omega_a) + \Gamma_e^a + \Gamma_\alpha^a} - \frac{\Gamma_e^s}{i(\omega - \omega_s) + \Gamma_e^s + \Gamma_\alpha^s}$ and

$r = S_{(U_1,U_1)} = \frac{\Gamma_e^a}{i(\omega - \omega_a) + \Gamma_e^a + \Gamma_\alpha^a} - \frac{\Gamma_e^s}{i(\omega - \omega_s) + \Gamma_e^s + \Gamma_\alpha^s}$. At the on-resonance condition

$\omega = \omega_a = \omega_s$, the requirement of $t, r = 0$ leads to

$$\Gamma_e^s \Gamma_e^a = \Gamma_\alpha^s \Gamma_\alpha^a, \quad (5-1)$$

$$\frac{\Gamma_e^s}{\Gamma_e^a} = \frac{\Gamma_\alpha^s}{\Gamma_\alpha^a}. \quad (5-2)$$

In Fig. 2(b), the PA (red star) is generated at the intersection between the nodal lines of t -SPS and r -SPS, where the degenerate critical coupling condition [54] is satisfied ($\Gamma_\alpha^a = \Gamma_e^a, \Gamma_\alpha^s = \Gamma_e^s$). Assuming $\Gamma_\alpha^s > \Gamma_\alpha^a$, one can observe +1 t -SPSs located in both $\omega - \Gamma_e^a / \Gamma_\alpha^a$ and $\omega - \Gamma_e^s / \Gamma_\alpha^s$ spaces [Fig. 2(c), left], while the reflection singularity has a topological charge of +1 in $\omega - \Gamma_e^a / \Gamma_\alpha^a$ space but -1 in $\omega - \Gamma_e^s / \Gamma_\alpha^s$ space [Fig. 2(c), right]. PA occurs when two nodal lines intersect, creating a *degenerate singularity*. Using Eq. (4), one can obtain $\tilde{\nu} = \nu_r + \nu_t = +1 + (+1) = +2$ in $\omega - \Gamma_e^a / \Gamma_\alpha^a$ space ($p_r, q_t = +1$) and $\tilde{\nu} = \nu_r - \nu_t = -1 - (+1) = -2$ in $\omega - \Gamma_e^s / \Gamma_\alpha^s$ space ($p_r = +1, q_t = -1$) considering the phase of $\varphi_{r \times t} = \arg(r \times t)$ [Fig. 2(d), left] and $\varphi_{r/t} = \arg(r/t)$ [Fig. 2(d), right], respectively. In other words, in a two-port system, the appearance of PA corresponds to the generation of ± 2 -order SPSs. When more channels are involved, the appearance of PA should be associated with high-order degenerate SPSs.

Next, we will give actual examples to demonstrate the underlying topological behaviors of PA, which empowers new opportunities to design perfect absorbers with more diversity. Fig. 3(a) shows a MIM structure with 1D Au gratings (period p , width w , and thickness h) adopted from Ref. [55]. The absorption enhancement can be realized by properly exciting magnetic polaritons within the dielectric interlayer (height H). For a given Au grating ($p = 400$ nm, $w = 250$ nm, $h = 20$ nm), by sweeping the reflection phase in $\lambda - H$ space under p -polarization, a +1 SPS in Fig. 3(b) with perfect absorption spectrum in Fig. 3(c) can be obtained. Such an individual SPS (or PA) will be topologically robust unless large parameter changes are introduced in the system (Fig. S6), which has not been uncovered before. Based on the charge conservation of SPSs, here we can propose a direct and simple method to achieve dual-band PA. The existing dual-band or multi-band absorbers mainly rely on either combining two or more resonators with different geometric sizes to form a super unit [36–39,56] or stack multilayer [40,57] with separated resonant frequencies. Such designs are more demanding for nanofabrication technologies, and it may be difficult to ensure unity absorptivity for all peaks simultaneously. Instead, the intrinsically topological nature of

PA will provide a new platform to overcome these challenges as sketched in Fig. 3(d). Considering a non-perfect absorption spectrum that may be ascribed to the annihilation of two SPSs [Fig. 1(g)], it in turn provides an opportunity to revive these singularities by tuning the balance between radiative and non-radiative loss of the whole system. For instance, at $H=25$ nm, there are no visible SPSs in $\lambda - p$ space [Fig. 3(e), left], because the structures do not satisfy the critical coupling condition. By increasing the Au grating's thickness (reducing the magnitude of radiative loss), two SPSs with opposite topological invariants emerge [Fig. 3(e), right], thus enabling dual-band PA in Fig. 3(f) (green line). As such, for different H far away from the red star in Fig. 3(b), one can always obtain dual-peak PA spectra using the above approach. In these cases, PA can be ensured all the time, and the spectral distance between two PA peaks can be flexibly tailored by shaping the positions of two SPSs. The intrinsic topological nature of PA-related SPSs governs the evolution of absorption spectra. The proposed method is also applicable to other systems with distinct advantages like maintaining robust, perfect absorption performance, releasing complex structure requirements and providing universal design principles (Note 3 [34]).

In Fig. 4, we show the topological behavior of SPSs for an all-dielectric absorber which consists of periodic a-Si ($\epsilon_{aSi} = 3.43 + i0.09$) nano-disks sitting on a glass ($\epsilon_g = 1.46$) substrate. The co-existence and destructive interference of electric (approximately symmetric) and magnetic (approximately asymmetric) resonances ensure the complete cancellation of both reflection and transmission. The period $p_x = p_y$, height L , and diameter d contribute to shaping the competitive balance between material loss and radiative loss of two modes. Fig. 4(b) shows the absorption (black), reflection (blue), and transmission (red) spectra under an optimal condition ($p_x = 270$ nm, $L_0 = 62$ nm, and $d = 160$ nm), associated with a -1 r -SPS and a $+1$ t -SPS at $\lambda_0 = 0.48\mu\text{m}$ and L_0 [Fig. 4(b), top], respectively. Since the whole system is in-plane symmetric, the PA also becomes polarization-insensitive, ensuring the appearance of -

4-SPS ($N=4$ considering p and s waves) by viewing the phase of $\arg[(r_p / t_p) \times (r_s / t_s)]$ in Fig. 4(c). The appearance of two separated -2 SPSs is ascribed to the degeneracy of reflection (left, $v_{r_p} + v_{r_s}$) or transmission (right, $-v_{t_p} - v_{t_s}$) channels under two polarization states. Consistently, as for an individual polarization, a clear -2 SPSs ($\tilde{v} = v_{r_p} - v_{t_p}$) could be obtained [Fig. 4(d), middle]. Owing to the topological robustness of PA-related SPSs, this -2 SPS will always exist even though the geometric parameters is moderately changed. For example, as for the non-ideal cases of $p_x = 290$ nm and $p_x = 250$ nm in Fig. 4(c), the -2 SPSs can also be ensured by increasing [Fig. 4(d), top] or decreasing [Fig. 4(d), bottom] the value of d . Fig. 4(e) shows the continuous evolution of the selected perfect absorption spectra as the diameter of the nanodisk changes, where PA can always be realized. In contrast, the majority of reported all-dielectric absorbers can only work at a specific wavelength [54,58–61]. Even though another PA may also be found by sparing no effort to sweep the geometric parameters, the underlying topology behavior behind the continuous evolution of PA has not been fully understood.

The above perfect absorption properties are discussed under normal incidence, but there are also several works paying attention to off- 0° performance. In analogy with accidental BICs [53,62–64], the existence of off- 0° PA does not require fine-tuning of system parameters. The small changes in parameters simply shift the position of these PA points, which are ascribed to the topological robustness of SPSs. In Note 4 [34], we consider a one-port structure composed of upper polar material and dielectric interlayer in Fig. S9. Around the epsilon-near-pole (ENP) wavelength, one can expect several SPSs in the reflection phase under two polarizations, owing to the interference effects between Fabry-Perot resonances and ENP modes. For both ± 1 and ± 2 (polarization-insensitive PA) SPSs, the charge conservation governs the whole evolution and annihilation processes.

Up to now, we have established the connections between PA and SPSs with

different topological invariants, including ± 1 , ± 2 , and even ± 4 (Table S1). Then, it is logical to think of the possibility of creating other quantized winding numbers of SPSs. One possible way is to consider high-order diffraction channels (i.e., $s_{U_0,+} = 1, s_{U_{\pm 1},+} = 0, s_{U_{\pm 1},-}, s_{U_0,-}$) in Note 5 [34]. But the pre-assumption of orthogonal modes always leads to $\text{Re}[S_{(U_0, U_{\pm 1})}] > 0$, the ± 1 -order diffraction cannot be desirably eliminated under this situation. Instead, one can consider exciting several non-orthogonal modes by using asymmetric meta-atoms [41]. In analogy with coherent perfect absorption [20], it is also possible to consider more than one input channels (i.e., $\tilde{r}_{\pm 1} \neq 0$), which can be expected to find more intriguing phenomena.

In conclusion, we have demonstrated that PA are associated with phase vortices in spectral spaces and reveal their topological behaviors in terms of conserved topological invariants related to SPSs. The intrinsic connection of SPSs' evolution between radiative loss and materials loss has been unambiguously established, and incorporated with the generation principles of high-order SPSs. Then, we re-interpret two basic types of absorbers from the prospects of topology, well explaining the robustness and evolution of absorption spectra as the system parameters change and proposing a novel strategy to design perfect dual-band absorbers. Our findings connect all the PA phenomena to a wide range of topological defects, vortex physics, phase modulation, etc. We believe that the revealed topological nature in scattering systems and related singular properties will breathe the traditional areas of absorbers/emitters and offers new opportunities in topological metasurfaces [65] or exception-points-related physics [66].

Acknowledgment

C.Y. Z. acknowledges the National Natural Science Foundation of China (No. 52120105009 and No. 51906144) and the Shanghai Key Fundamental Research Grant (No. 20JC1414800). C.-W. Q. acknowledges the financial support of the Ministry of Education, Republic of Singapore (Grant No. R-263-000-E19-114). M. Q. L. acknowledges the support from China Postdoctoral Science Foundation (No.

BX20220200) and the SJTU-NUS Joint PhD Project. S. F. acknowledges the support of U. S. Department of Energy (Grant No. DE-FG02-07ER46426)).

Author Contributions

M.Q.L and C.-W. Q. conceived the ideas. M.Q.L developed the theory and performed the simulations. M.Q.L., W.J.C., G.W.H., S. F., D.N.C, C.Y.Z. and C-W.Q. analyzed the data and all authors discussed the results. M.Q.L. wrote the manuscript with inputs and comments from all authors. C.Y.Z. and C-W.Q. supervised the project.

Competing interests

The authors declare no competing interests.

Data and materials availability

All associated data and materials are available in the manuscript and supplementary materials.

Supplementary Materials

Note 1: Temporal coupled-mode theory and generation of spectral phase singularity

Note 2: High-order spectral phase singularity (SPS) in two-port-two-mode systems

Note 3: Comparison of existing methods for dual-band absorbers

Note 4: Spectral phase singularity at off- θ° : incline incident

Note 5: Possibility of spectral phase singularity with other orders

Figure S1-S9, Table S1

References

- [1] D. Gevaux, *Perfect Heat*, Nature Physics **7**, 670 (2011).
- [2] V. S. Asadchy, I. A. Faniayeu, Y. Ra'di, S. A. Khakhomov, I. V. Semchenko, and S. A. Tretyakov, *Broadband Reflectionless Metasheets: Frequency-Selective Transmission and Perfect Absorption*, Physical Review X **5**, 031005 (2015).
- [3] I. E. Khodasevych, L. Wang, A. Mitchell, and G. Rosengarten, *Micro- and Nanostructured Surfaces for Selective Solar Absorption*, Advanced Optical Materials **3**, 852 (2015).
- [4] R. Alaei, M. Albooyeh, and C. Rockstuhl, *Theory of Metasurface Based Perfect Absorbers*, Journal of Physics D: Applied Physics **50**, 503002 (2017).
- [5] M. Liu and C. Zhao, *Ultranarrow and Wavelength-Scalable Thermal Emitters Driven by High-Order Antiferromagnetic Resonances in Dielectric Nanogratings*, ACS Applied

- Materials & Interfaces **13**, 25306 (2021).
- [6] D. G. Baranov, Y. Xiao, I. A. Nechepurenko, A. Krasnok, A. Alù, and M. A. Kats, *Nanophotonic Engineering of Far-Field Thermal Emitters*, Nature Materials **18**, 920-930, (2019).
- [7] B. X. Wang, Y. He, P. Lou, and W. Xing, *Design of a Dual-Band Terahertz Metamaterial Absorber Using Two Identical Square Patches for Sensing Application*, Nanoscale Advances **2**, 763 (2020).
- [8] D. M. Bierman, A. Lenert, W. R. Chan, B. Bhatia, I. Celanović, M. Soljačić, and E. N. Wang, *Enhanced Photovoltaic Energy Conversion Using Thermally Based Spectral Shaping*, Nature Energy **1**, 16068 (2016).
- [9] A. Lenert, D. M. Bierman, Y. Nam, W. R. Chan, I. Celanović, M. Soljačić, and E. N. Wang, *A Nanophotonic Solar Thermophotovoltaic Device*, Nature Nanotechnology **9**, 126 (2014).
- [10] D. Fan, T. Burger, S. McSherry, B. Lee, A. Lenert, and S. R. Forrest, *Near-Perfect Photon Utilization in an Air-Bridge Thermophotovoltaic Cell*, Nature **586**, 237 (2020).
- [11] A. Tittl, A. K. U. Michel, M. Schäferling, X. Yin, B. Gholipour, L. Cui, M. Wuttig, T. Taubner, F. Neubrech, and H. Giessen, *A Switchable Mid-Infrared Plasmonic Perfect Absorber with Multispectral Thermal Imaging Capability*, Advanced Materials **27**, 4597 (2015).
- [12] N. I. Landy, C. M. Bingham, T. Tyler, N. Jokerst, D. R. Smith, and W. J. Padilla, *Design, Theory, and Measurement of a Polarization-Insensitive Absorber for Terahertz Imaging*, Physical Review B **79**, 125104 (2009).
- [13] F. Zhang, C. Li, Y. Fan, R. Yang, N.-H. Shen, Q. Fu, W. Zhang, Q. Zhao, J. Zhou, T. Koschny et al., *Phase-Modulated Scattering Manipulation for Exterior Cloaking in Metal–Dielectric Hybrid Metamaterials*, Advanced Materials **31**, 1903206 (2019).
- [14] A. Berkhout and A. F. Koenderink, *Perfect Absorption and Phase Singularities in Plasmon Antenna Array Etalons*, ACS Photonics **6**, 2917 (2019).
- [15] Y. X. Yeng, M. Ghebrehan, P. Bermel, W. R. Chan, J. D. Joannopoulos, M. Soljačić, and I. Celanovic, *Enabling High-Temperature Nanophotonics for Energy Applications*, Proceedings of the National Academy of Sciences of the United States of America **109**, 2280 (2012).
- [16] P. Huo, S. Zhang, Y. Liang, Y. Lu, and T. Xu, *Hyperbolic Metamaterials and Metasurfaces: Fundamentals and Applications*, Advanced Optical Materials **7**, 1801616 (2019).
- [17] N. Liu, M. Mesch, T. Weiss, M. Hentschel, and H. Giessen, *Infrared Perfect Absorber and Its Application as Plasmonic Sensor*, Nano Letters **10**, 2342 (2010).
- [18] C. T. Riley, J. S. T. Smalley, J. R. J. Brodie, Y. Fainman, D. J. Sirbully, and Z. Liub, *Near-Perfect Broadband Absorption from Hyperbolic Metamaterial Nanoparticles*, Proceedings of the National Academy of Sciences of the United States of America **114**, 1264 (2017).
- [19] C. Y. Yang, J. H. Yang, Z. Y. Yang, Z. X. Zhou, M. G. Sun, V. E. Babicheva, and K. P. Chen, *Nonradiating Silicon Nanoantenna Metasurfaces as Narrowband Absorbers*, ACS Photonics **5**, 2596 (2018).
- [20] C. Wang, W. R. Sweeney, A. D. Stone, and L. Yang, *Coherent Perfect Absorption at an Exceptional Point*, Science **373**, 1261 (2021).
- [21] S. Zano, F. P. Mezzapesa, F. Bianco, G. Biasiol, L. Baldacci, M. S. Vitiello, L. Sorba, R. Colombelli, and A. Tredicucci, *Perfect Energy-Feeding into Strongly Coupled Systems and Interferometric Control of Polariton Absorption*, Nature Physics **10**, 830 (2014).
- [22] K. V. Sreekanth, S. Han, and R. Singh, *Ge₂Sb₂Te₅-Based Tunable Perfect Absorber Cavity*

- with Phase Singularity at Visible Frequencies*, *Advanced Materials* **30**, 1706696 (2018).
- [23] V. G. Kravets, F. Schedin, R. Jalil, L. Britnell, R. V. Gorbachev, D. Ansell, B. Thackray, K. S. Novoselov, A. K. Geim, A. V. Kabashin et al., *Singular Phase Nano-Optics in Plasmonic Metamaterials for Label-Free Single-Molecule Detection*, *Nature Materials* **12**, 304 (2013).
- [24] K. V. Sreekanth, S. Sreejith, S. Han, A. Mishra, X. Chen, H. Sun, C. T. Lim, and R. Singh, *Biosensing with the Singular Phase of an Ultrathin Metal-Dielectric Nanophotonic Cavity*, *Nature Communications* **9**, 369 (2018).
- [25] Y. Tsurimaki, J. K. Tong, V. N. Boriskin, A. Semenov, M. I. Ayzatsky, Y. P. Machekhin, G. Chen, and S. V. Boriskina, *Topological Engineering of Interfacial Optical Tamm States for Highly Sensitive Near-Singular-Phase Optical Detection*, *ACS Photonics* **5**, 929 (2018).
- [26] Y. Bai, H. Zheng, Q. Zhang, Y. Yu, and S. Liu, *Perfect Absorption and Phase Singularities Induced by Surface Lattice Resonances for Plasmonic Nanoparticle Array on a Metallic Film*, *Optics Express* **30**, 45400 (2022).
- [27] Z. Sakotic, A. Krasnok, A. Alú, and N. Jankovic, *Topological Scattering Singularities and Embedded Eigenstates for Polarization Control and Sensing Applications*, *Photonic Research* **9**, 1310 (2021).
- [28] G. Ermolaev, K. Voronin, D. G. Baranov, V. Kravets, G. Tselikov, Y. Stebunov, D. Yakubovsky, S. Novikov, A. Vyshnevyy, A. Mazitov et al., *Topological Phase Singularities in Atomically Thin High-Refractive-Index Materials*, *Nature Communications* **13**, 2049 (2022).
- [29] P. A. Thomas, K. S. Menghrajani, and W. L. Barnes, *All-Optical Control of Phase Singularities Using Strong Light-Matter Coupling*, *Nature Communications* **13**, 1 (2022).
- [30] S. M. Hein and H. Giessen, *Retardation-Induced Phase Singularities in Coupled Plasmonic Oscillators*, *Physical Review B* **91**, 205402 (2015).
- [31] M. Liu, C. Zhao, Y. Zeng, Y. Chen, C. Zhao, and C. Qiu, *Evolution and Nonreciprocity of Loss-Induced Topological Phase Singularity Pairs*, *Physical Review Letters* **127**, 266101 (2021).
- [32] W. Suh and S. Fan, *All-Pass Transmission or Flattop Reflection Filters Using a Single Photonic Crystal Slab*, *Applied Physics Letters* **84**, 4905 (2004).
- [33] W. Suh, Z. Wang, and S. Fan, *Temporal Coupled-Mode Theory and the Presence of Non-Orthogonal Modes in Lossless Multimode Cavities*, *IEEE Journal of Quantum Electronics* **40**, 1511 (2004).
- [34] See Supplementary Material at <http://...> for notes: 1. Temporal coupled-mode theory and generation of spectral phase singularity; 2. High-order spectral phase singularity (SPS) in two-port-two-mode systems; 3. Comparison of existing methods for dual-band absorbers; 4. Spectral phase singularity at off- 0° : incline incident; 5. Possibility of spectral phase singularity with other orders. The supplemental Material also contains Ref. [35-41].
- [35] J. R. Hendrickson, S. Vangala, C. Dass, R. Gibson, J. Goldsmith, K. Leedy, D. E. Walker, J. W. Cleary, W. Kim, and J. Guo, *Coupling of Epsilon-Near-Zero Mode to Gap Plasmon Mode for Flat-Top Wideband Perfect Light Absorption*, *ACS Photonics* **5**, 776 (2018).
- [36] K. Chen, R. Adato, and H. Altug, *Dual-Band Perfect Absorber for Multispectral Plasmon-Enhanced Infrared Spectroscopy*, *ACS Nano* **6**, 7998 (2012).
- [37] B. Zhang, Y. Zhao, Q. Hao, B. Kiraly, I.-C. Khoo, S. Chen, and T. J. Huang, *Polarization-Independent Dual-Band Infrared Perfect Absorber Based on a Metal-Dielectric-Metal*

- Elliptical Nanodisk Array*, Optics Express **19**, 15221 (2011).
- [38] X. Liu, T. Tyler, T. Starr, A. F. Starr, N. M. Jokerst, and W. J. Padilla, *Taming the Blackbody with Infrared Metamaterials as Selective Thermal Emitters*, Physical Review Letters **107**, 045901 (2011).
- [39] J. Liu, M. Zhu, N. Zhang, H. Zhang, Y. Zhou, S. Sun, N. Yi, S. Gao, Q. Song, and S. Xiao, *Wafer-Scale Metamaterials for Polarization-Insensitive and Dual-Band Perfect Absorption*, Nanoscale **7**, 18914 (2015).
- [40] Y. H. Kan, C. Y. Zhao, X. Fang, and B. X. Wang, *Designing Ultrabroadband Absorbers Based on Bloch Theorem and Optical Topological Transition*, Optics Letters **42**, 1879 (2017).
- [41] Z. Fan, M. R. Shcherbakov, M. Allen, J. Allen, B. Wenner, and G. Shvets, *Perfect Diffraction with Multiresonant Bianisotropic Metagratings*, ACS Photonics **5**, 4303 (2018).
- [42] B. X. Wang, M. Q. Liu, T. C. Huang, and C. Y. Zhao, *Micro/Nanostructures for Far-Field Thermal Emission Control: An Overview*, ES Energy & Environment **6**, 18 (2019).
- [43] W. Li and S. Fan, *Nanophotonic Control of Thermal Radiation for Energy Applications [Invited]*, Optics Express **26**, 15995 (2018).
- [44] J. Wang, A. Chen, Y. Zhang, J. Zeng, Y. Zhang, X. Liu, L. Shi, and J. Zi, *Manipulating Bandwidth of Light Absorption at Critical Coupling: An Example of Graphene Integrated with Dielectric Photonic Structure*, Physical Review B **100**, 075407 (2019).
- [45] C. Qu, S. Ma, J. Hao, M. Qiu, X. Li, S. Xiao, Z. Miao, N. Dai, Q. He, S. Sun et al., *Tailor the Functionalities of Metasurfaces Based on a Complete Phase Diagram*, Physical Review Letters **115**, 235503 (2015).
- [46] W. Chen, Q. Yang, Y. Chen, and W. Liu, *Evolution and Global Charge Conservation for Polarization Singularities Emerging from Non-Hermitian Degeneracies*, Proceedings of the National Academy of Sciences of the United States of America **118**, 1 (2021).
- [47] B. Zhen, C. W. Hsu, L. Lu, A. D. Stone, and M. Soljačić, *Topological Nature of Optical Bound States in the Continuum*, Physical Review Letters **113**, 257401 (2014).
- [48] Y. Guo, M. Xiao, and S. Fan, *Topologically Protected Complete Polarization Conversion*, Physical Review Letters **119**, 1 (2017).
- [49] N. D. Mermin, *The Topological Theory of Defects in Ordered Media*, Reviews of Modern Physics **51**, 591 (1979).
- [50] M. Zürch, C. Kern, P. Hansinger, A. Dreischuh, and C. Spielmann, *Strong-Field Physics with Singular Light Beams*, Nature Physics **8**, 743 (2012).
- [51] L. Du, A. Yang, A. V. Zayats, and X. Yuan, *Deep-Subwavelength Features of Photonic Skyrmions in a Confined Electromagnetic Field with Orbital Angular Momentum*, Nature Physics **15**, 650 (2019).
- [52] Y. Wang, Z.-L. Deng, D. Hu, J. Yuan, Q. Ou, F. Qin, Y. Zhang, X. Ouyang, Y. Li, B. Peng et al., *Atomically Thin Noble Metal Dichalcogenides for Phase-Regulated Meta-Optics*, Nano Letters **20**, 7811 (2020).
- [53] M. Kang, S. Zhang, M. Xiao, and H. Xu, *Merging Bound States in the Continuum at Off-High Symmetry Points*, Physical Review Letters **126**, 117402 (2021).
- [54] J. R. Piper, V. Liu, and S. Fan, *Total Absorption by Degenerate Critical Coupling*, Applied Physics Letters **104**, 251110 (2014).
- [55] S. Y. Chou, *$\lambda^3/1000$ Plasmonic Nanocavities for Biosensing Fabricated by Soft UV Nanoimprint Lithography*, Nano Letters **11**, 3557 (2012).

- [56] Y. Xiang, L. Wang, Q. Lin, S. Xia, M. Qin, and X. Zhai, *Tunable Dual-Band Perfect Absorber Based on L-Shaped Graphene Resonator*, IEEE Photonics Technology Letters **31**, 483 (2019).
- [57] S. Liu, H. Chen, and T. J. Cui, *A Broadband Terahertz Absorber Using Multi-Layer Stacked Bars*, Applied Physics Letters **106**, 1 (2015).
- [58] X. Ming, X. Liu, L. Sun, and W. J. Padilla, *Degenerate Critical Coupling in All-Dielectric Metasurface Absorbers*, Optics Express **25**, 24658 (2017).
- [59] H. Li, G. Wei, H. Zhou, H. Xiao, M. Qin, S. Xia, and F. Wu, *Polarization-Independent near-Infrared Superabsorption in Transition Metal Dichalcogenide Huygens Metasurfaces by Degenerate Critical Coupling*, Physical Review B **105**, 165305 (2022).
- [60] R. Xu and J. Takahara, *Radiative Loss Control of an Embedded Silicon Perfect Absorber in the Visible Region*, Optics Letters **46**, 805 (2021).
- [61] J. Yu, B. Ma, A. Ouyang, P. Ghosh, H. Luo, A. Pattanayak, S. Kaur, M. Qiu, P. Belov, and Q. Li, *Dielectric Super-Absorbing Metasurfaces via PT Symmetry Breaking*, Optica **8**, 1290 (2021).
- [62] M. S. Sidorenko, O. N. Sergaeva, Z. F. Sadrieva, C. Roques-Carmes, P. S. Muraev, D. N. Maksimov, and A. A. Bogdanov, *Observation of an Accidental Bound State in the Continuum in a Chain of Dielectric Disks*, Physical Review Applied **15**, 034041 (2021).
- [63] X. Zhao, C. Chen, K. Kaj, I. Hammock, Y. Huang, R. D. Averitt, and X. Zhang, *Terahertz Investigation of Bound States in the Continuum of Metallic Metasurfaces*, Optica **7**, 1548 (2020).
- [64] T. Yoda and M. Notomi, *Generation and Annihilation of Topologically Protected Bound States in the Continuum and Circularly Polarized States by Symmetry Breaking*, Physical Review Letters **125**, 53902 (2020).
- [65] C. W. Qiu, T. Zhang, G. Hu, and Y. Kivshar, *Quo Vadis, Metasurfaces?*, Nano Letters **21**, 5461 (2021).
- [66] Q. Song, M. Odeh, J. Zúñiga-Pérez, B. Kanté, and P. Genevet, *Plasmonic Topological Metasurface by Encircling an Exceptional Point*, Science **373**, 1133 (2021).

Figures

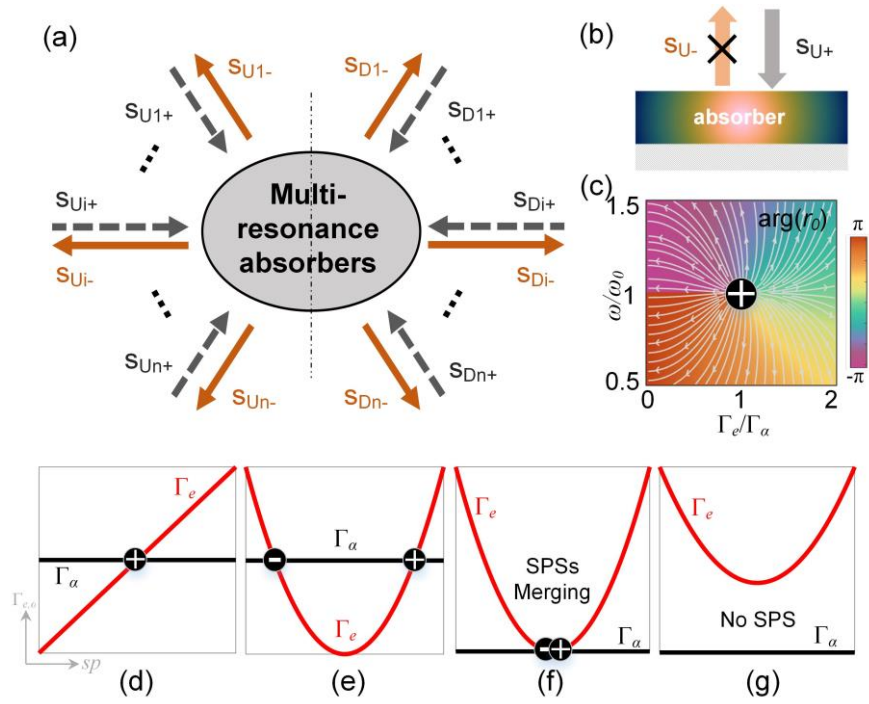


Fig. 1 Topological nature of PA points associated with SPSs. (a) Schematic of the multi-port multi-mode system. The subscript “U” and “D” denote the upper and downside channels. (b) The mirror-backed one-port system, along with (c) its typical reflection phase in parameter space. (d)-(g) Possible relations between radiative loss Γ_e and material loss Γ_α at $\omega = \omega_0$: linear type for all Γ_α ; linear type for Γ_e in (d) and hyperbolic type for Γ_e in (e)-(g). The “ sp ” could represent the system parameter, like thickness, period, incident angle, etc.

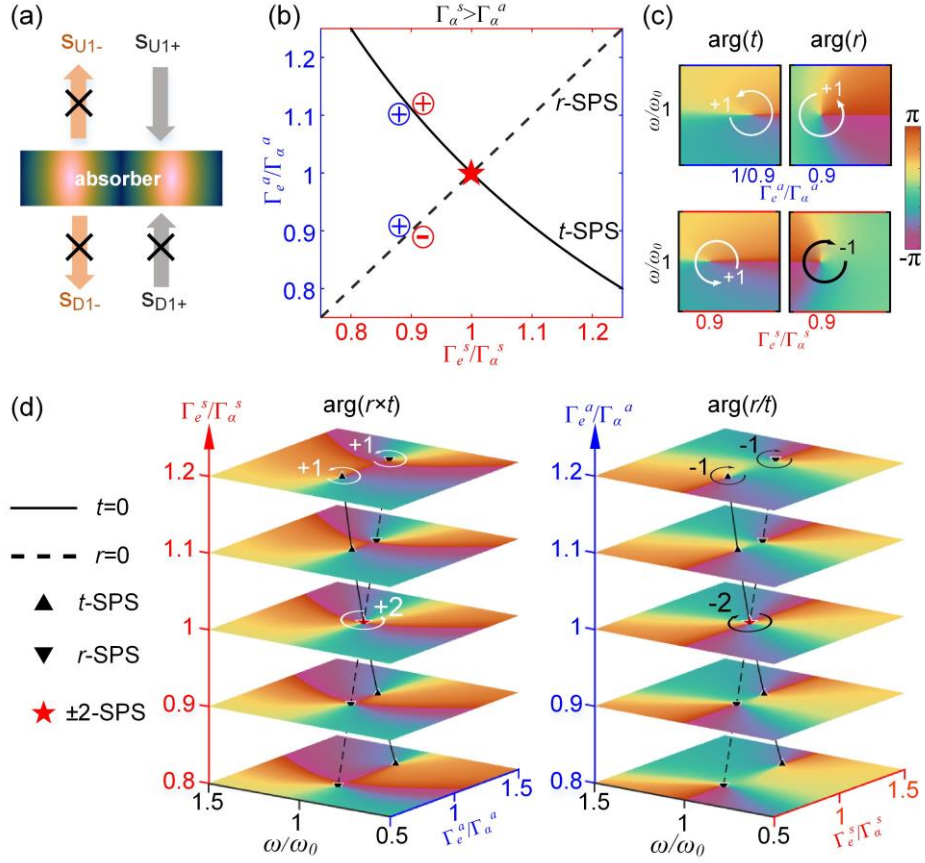


Fig. 2 High-order PA-related SPSs. (a) Schematic of the two-port system. (b) Evolution trajectory of reflection-type SPSs ($r = 0$, dashed line) and transmission-type SPSs ($t = 0$, full line). The red pentagram denotes the position of PA point. The topological charges are marked in different projection planes: $\omega - \Gamma_e^a / \Gamma_\alpha^a$ space (blue) and $\omega - \Gamma_e^s / \Gamma_\alpha^s$ space (red), along with (c) the corresponding reflection or transmission phase. (d) Generation rules of high-order SPSs viewing the phase of $\varphi_{r \times t} = \arg(r \times t)$ in $\omega - \Gamma_e^a / \Gamma_\alpha^a$ space (left) and $\varphi_{r/t} = \arg(r / t)$ in $\omega - \Gamma_e^s / \Gamma_\alpha^s$ space (right).

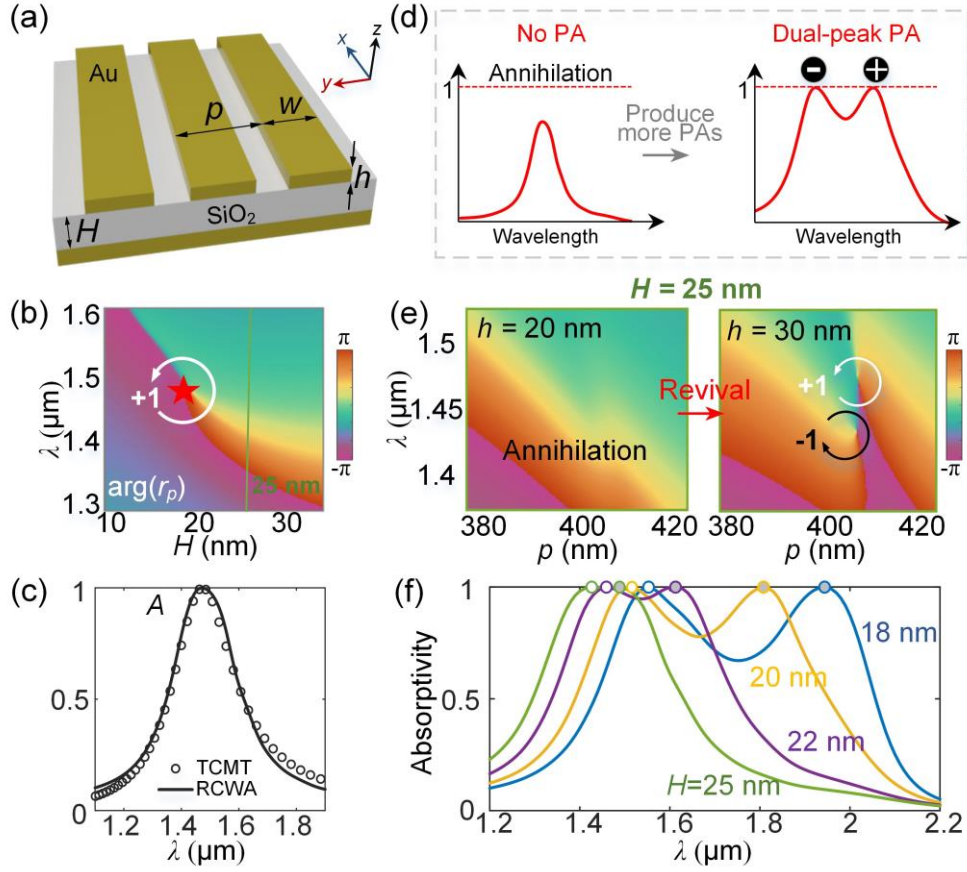


Fig. 3 Topological behaviors of SPSs in MIM perfect absorbers. (a) Schematic of the MIM absorber, composed of a bottom Au mirror, SiO₂ interlayer, and Au gratings. The p -polarization (E_x, H_y, k_z) is considered. (b) Reflection phase (φ_{r_0}) viewing in $\lambda-H$ space. The +1 SPS is denoted with a red star, along with (c) the corresponding perfect absorption spectrum ($H=18$ nm). (d) A design principle for dual-band perfect absorbers based on the charge evolution of topological phase singularity: (Left) no PA with annihilated SPSs and (Right) dual-peak PA points with two revival SPSs. (e) Typical cases for presenting the evolution of SPSs in $\lambda-p$ space, at $H = 25$ nm and different h . (f) Absorption spectra with dual PA peaks for cases with different H , were obtained based on the method in (d). The circles in white or gray represent PA points associated with -1 or +1 SPSs in $\lambda-p$ space.

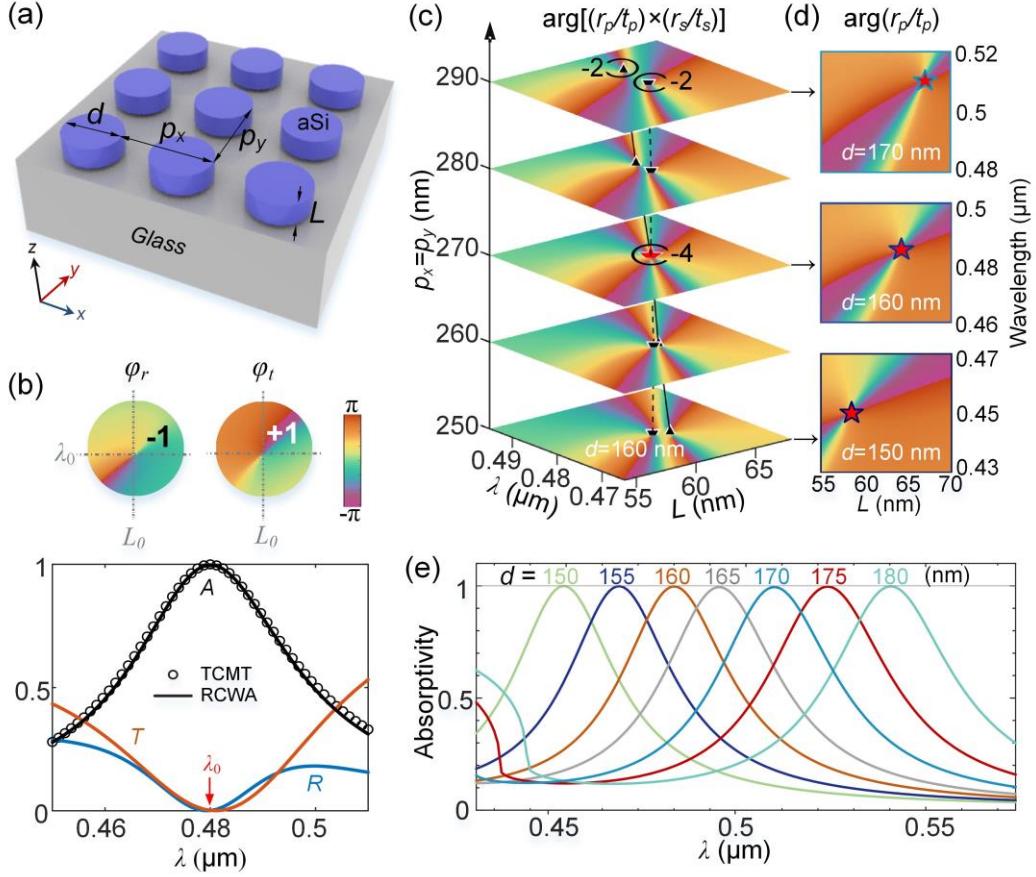


Fig. 4 Topological behaviors of high-order SPSs in all-dielectric perfect absorbers. (a) Schematic of the all-dielectric absorber, composed of periodic a-Si nano-disks sitting on a glass substrate. (b) Absorption (black), reflection (blue), and transmission (red) spectra, together with the phase φ_r ($\nu = -1$) and φ_t ($\nu = +1$) in $\lambda - L$ space. The λ_0 denotes the wavelength of PA point. (c) Generation of high-order SPSs in the phase of $\arg\left[\left(r_p/t_p\right) \times \left(r_s/t_s\right)\right]$ changing with different p_x at a fixed $d = 160$ nm. (d) Three typical phases of $\arg\left(r_p/t_p\right)$: (top) $p_x = 290$ nm, $d = 170$ nm, (middle) $p_x = 270$ nm, $d = 160$ nm, and (bottom) $p_x = 250$ nm, $d = 150$ nm. (e) Topological robustness of high-order SPSs: absorption spectra with PA peaks as the diameter d changes.